Power measurements and coupler optimization in inductive discharges

V. A. Godyak and , and B. M. Alexandrovich

Citation: Review of Scientific Instruments **88**, 083512 (2017); doi: 10.1063/1.4995810
View online: http://dx.doi.org/10.1063/1.4995810
View Table of Contents: http://aip.scitation.org/toc/rsi/88/8
Published by the American Institute of Physics

REVIEW OF SCIENTIFIC INSTRUMENTS **88**, 083512 (2017)

Power measurements and coupler optimization in inductive discharges

V. A. Godyak[1,a)] and B. M. Alexandrovich[2]
[1]*Electrical Engineering and Computer Science Department, University of Michigan, Ann Arbor, Michigan 48109, USA and RF Plasma Consulting, Brookline, Massachusetts 02446, USA*
[2]*Plasma Sensors, Brookline, Massachusetts 02446, USA*

(Received 9 January 2017; accepted 12 July 2017; published online 21 August 2017)

The power absorbed by the plasma is one of the key parameters which defines processes in any plasma source. This power, however, can be very different from the power at the rf power source output or the coupler terminals, which has been used in many publications to characterize the plasma. This article describes how to find the power absorbed by the plasma and the power lost in the coupler and matcher network for inductively coupled plasmas. In addition, several practical coupler configurations to reduce the coupler coil loss and minimize the rf plasma potential are discussed. We propose an effective and simple method to achieve that by the coupler coil splitting and insertion of the resonating capacitor in the middle of the coil. Our experimental data demonstrate this approach having superior coupler efficiency and substantially lower rf plasma potential. *Published by AIP Publishing.* [http://dx.doi.org/10.1063/1.4995810]

Inductively coupled plasma (ICP) sources have several distinct advantages over other rf plasma sources. In the ICP, the plasma density control is independent of the substrate bias, and its rf and dc plasma potentials are usually low. The properly designed ICPs enhanced with ferromagnetic core[1] have coupler power loss an order of magnitude less than the most efficient helicon plasma sources.[2] The latter have to be supplemented by the magnet assembly, thus, further compromising the plasma system efficiency and its cost.

The unique feature of ICP is its ability to operate in a wide range of frequencies from tens of Hz[3] up to GHz.[4] While many research and industrial ICPs operate at 13.56 MHz, there are significant advantages of the ICP operation in 0.4–4 MHz frequency range. Lower frequency brings benefits of higher efficiency, better control over the discharge power, and more reliable measurements of ICP electrical parameters, while reducing the rf equipment cost.

The ICP resembles a conventional ac transformer with the primary multi- or single-turn coil (named interchangeably in shop jargon—an antenna, an induction coil, a coupler coil, or a coupler) and a single-turn secondary comprising a toroidal rf current.

In a conventional transformer, the coupling coefficient, k, between the primary and the secondary windings is close to unity, $k \approx 1$, and voltage, V, and current, I, ratios of primary and secondary circuits are $V_1/V_2 = I_2/I_1 = N_1/N_2 = N$. In the case of ICP, this coupling is often weak, and the coupling coefficient is essentially less than unity ($k < 1$), resulting that the voltage and current induced in the plasma are less than that defined by the turn ratio, i.e., $V_2 \equiv V_p < V_1/N$ and $I_2 \equiv I_p < I_1 N$. Here N is the number of turns in the ICP coupler coil.

Loose coupling between the inductor coil and the plasma, as well as the coil loss limit power transfer efficiency, $\eta = P_p/P_t$ of conventional ICP with the air core inductor. Here, P_p is the power deposited into the plasma, P_t is the power transmitted to the coupler coil, $P_t = P_p + P_c$, and P_c is the power loss in the coil. Therefore, the rf power deposited into plasma is always less than the power measured at the coil terminals. If the power is measured at the rf generator output, P_g, then additional losses in the matcher and transmission line (cable) should be taken into account. The difficulty for such assessment comes from the plasma being a non-linear load; its rf impedance $Z_p = V_p/I_p$ depends on absorbed power. That makes invalid assumptions of the coupler and matcher loss being proportional to the plasma power.

There is a simple and reliable method for measuring the plasma power, P_p, based on the transformer model of ICP, introduced and used by the authors in the past,[5–7] but ignored in industry and in majority of papers on this subject. This method does not require a perfect tuning and matching of the coupler circuit, although these procedures simplify measurements and maximize power utilization of the rf generator.

A simple equivalent circuit shown in Fig. 1(a) is a valid representation of the coupler coil loaded by the plasma.[5] There, L is the coupler coil inductance, R_0 is the coil resistance, and R_p is the plasma resistance transformed into the primary. Due to final plasma impedance transformed to the primary, the equivalent inductance, L, is somewhat smaller than the coil self-inductance, L_0.

The coil rf resistance, R_o, is significantly higher than the one measured by the ohmmeter due to skin and proximity effects. The impact of the later originated from the magnetic coupling between the coil adjacent turns may considerably prevail. Losses by eddy currents induced in chamber metal parts, which are in close proximity to the coil, further contribute to Ro. The coil inter-winding capacitance and its stray capacitance to the ground also affect R_o. Their impact gets most pronounced at frequencies approaching the coil self-resonance.

According to Ref. 5, the plasma resistance transformed to the primary is defined by the following expression:

a)egodyak@comcast.net

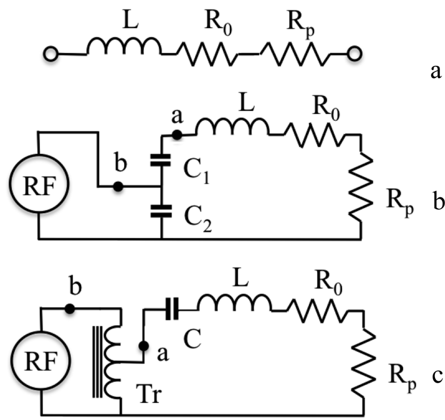

FIG. 1. Equivalent circuits of (a) a coupler coil not loaded with plasma, (b) the coupler capacitive matching to the rf source, (c) the coupler transformer matching to the rf source.

$$R_p = \frac{k^2\omega^2 L_0 R_2}{Z_2^2}, \text{ where } Z_2^2 = (\omega L_2 + R_2\frac{\omega}{\upsilon})^2 + R_2^2. \quad (1)$$

Here $\omega/2\pi = f$ is the driving frequency, and R_2, ωL_2, and Z_2 are, correspondingly, plasma turn resistance, magnetic reactance, and impedance. The magnetic reactance is defined by the geometry of the plasma current path, while $R_2\frac{\omega}{\upsilon}$ is the plasma reactance due to the electron inertia, and ν is the effective electron collision frequency defined by electron-atom collisions and collisionless power absorption due to electron thermal motion in the non-uniform rf field.

Calculating the correct R_p value from the above formula is impossible because its parameters are hard to define with any acceptable accuracy. But it can be found experimentally[5–7] by measuring the impedance change caused by the plasma load.

Measurements of the rf current and power at the coupler terminals allow us to find the power transferred to plasma P_p and assess the power loss in the coupler itself, P_c, and in the matcher, P_m. These measurements allow us to quantify the ICP performance in terms of the power transfer efficiency, $\eta = P_p/P_t$, and the power factor, $PF = \cos\phi$.

To find these parameters, the coil current, I_c, and the power delivered to the ICP coupler, $P_t = P_p + P_c$, have to be measured with and without plasma. Then, the power absorbed by the plasma, P_p, the power lost in the antenna coil, P_c, and the ICP power transfer efficiency, η, can be found as follows:

$$P_p = P_t - P_c, \; P_c = (I_c/I_{c0})^2 P_{c0}, \text{ and } \eta = P_p/P_t = R_p/(R_p + R_0), \quad (2)$$

where parameters indexed by 0 are measured without plasma.

There are few ways to measure the quantities of P_t and I_c, depending on the matching network which precedes the coupler. Two known examples of coupling the ICP coil to the power source are presented in Figs. 1(b) and 1(c). A matching network consisting of two capacitors, C_1 and C_2, is shown in Fig. 1(b). At certain values of C_1 and C_2, one can resonate the coupler coil at the driving frequency and match it to the generator. Precise tuning and matching can be achieved with variable capacitors C_1 and C_2, although it is more convenient to resonate the coupler inductance by adjusting the generator frequency, while having C_1, C_2 combination fixed near the optimal value.

The capacitive matching network [Fig. 1(b)] made of rf ceramic, air, or vacuum capacitors has negligible power loss, since the loss in the coupler coil exceeds the loss in such capacitors by nearly two orders of magnitude. Losses in conventional L, T, or Pi matching networks comprising an inductor should always be taken into account.

In the configuration shown in Fig. 1(b), the current into the coupler is measured at point **a**, and the power meter is connected to point **b**. Alternatively, the power at point **b** can be found as the mean value of the **V**(t)**I**(t) waveform product; this measurement can be performed with many digital oscilloscopes.

Another matching network connecting the ICP coupler to the generator is shown on Fig. 1(c). It was proposed in Ref. 8 and adopted in Refs. 6 and 7. Unlike Fig. 1(b) configuration, matching of this network is essentially independent from its tuning. Just two waveforms $\mathbf{I}_c$(t) and $\mathbf{V}_a$(t) acquired at point **a** contain full information of the network electrical characteristics. The power at point **a** could also be found as the generator power at point **b** minus the transformer loss.

Compact and extremely efficient (around 99%) step-down rf transformers utilizing features of the transmission line have been described in Ref. 9 and implemented for ICP matching.[6,7] In order to match the coupler to the rf generator this transformer could be wound with multiple outputs corresponding to different step-down ratios; having symmetrically wound outputs would further benefit the ICP drive.

Accurate evaluation of the coupler power loss is only possible at point **a** while the network is tuned close to resonance because the power measured directly at the coupler terminals is subjected to a significant error. This error is due to near orthogonal vectors of $\mathbf{V}_c$ and $\mathbf{I}_c$ at the coupler coil. The coupler loaded with plasma in typical ICP has Q-factor >10 when $\cos\phi \approx Q^{-1} \ll 1$. Then, the relative error in power measurement $\Delta P/P = \Delta\phi Q$, where $\Delta\phi$ is the absolute phase error in radian. For example, at $\Delta\phi = 0.0174 = 1°$, and $Q = 20$, the phase related error $\Delta P/P = 35\%$.

The ICP coupler is the essential part of the ICP system that defines the ICPs' power transfer efficiency and rf and dc plasma potentials. The ratio of the power delivered to plasma and power lost in the coupler, P_p/P_c, is proportional to k^2Q_0.[5] Efficient ICPs are only possible with low loss coils strongly coupled to plasma. Such couplers ensure stable operation at low plasma density (since the criterion of stable ICP operation is $P_p > P_c$), and they facilitate ignition and transition to the inductive mode. The highest Q-factor of the multi-turn unloaded coupler coil with an air core is achieved when the gap between adjacent turns is equal to the wire diameter, d.

The coupling coefficient of the coil to the plasma, k, is another parameter affecting ICP power efficiency. In cases of an air core coil, this coefficient depends on the coil distance from the plasma boundary, h, and the coil width, w. A greater w/h ratio leads to a higher value of the coupling coefficient, k.

An example of inefficient coupler design is a single turn coil occasionally used to minimize the coil voltage and, thus, to reduce rf and dc plasma potentials. In the case of a single-turn

or a narrow coil ($w \approx d$), the EMF induced at the plasma boundary is about $N(1 + 2h/d)$ times less than the coil voltage. That leads to an increase of the coil power loss, $P_c \propto I_c^2 \propto E_c^2$, by the factor $(1 + 2h/d)^2$ comparing to the ideal case of $h/d = 0$. Anticipated power loss of the single-turn coil wound with a 1/4 in. diameter copper tube separated from the plasma by 1/2 in. gap is about 25 times larger than that for the same coil when $k = 1$.

Single-turn coils have a lower Q-factor comparing to multi-turn coils. That can be explained by the following consideration: $Q_0 = \omega L/R_0$, and for short coil, $L \propto N^2$, while $R_0 \propto N$. Note that increasing the number of turns beyond a certain number (when the coil self-resonance frequency approaches the ICP driving frequency) may adversely affect the coil Q-factor.

The magnitude of induced rf plasma potential, V_0, due to the coil capacitance to the plasma is another important characteristic of ICP couplers. A high rf plasma potential, $V_0 > T_e/e$, produces an additional floating dc potential, thus increasing the minimal energy of the ions reaching the processing substrate and the chamber wall; the ion bombardment causes their erosion and the plasma contamination. A high rf plasma potential also distorts results of Langmuir, B-dot, and microwave probe diagnostics. Faraday shields applied to reduce the capacitive coupling between the coil and the plasma substantially increase rf power loss, impede the discharge breakdown, and its transition to the inductive mode.

The plasma rf potentials in ICP (and in Capacitively Coupled Discharge (CCP)) can be significantly reduced by the balanced (symmetrical) drive of the coupler.[10] The balanced drive significantly reduces the rf plasma potential at the fundamental frequency and odd harmonics, although the second harmonic is still present due to non-linearity of the window (or rf electrode) sheaths. When the coil drive is balanced, the dielectric window with a relatively high dielectric constant, ε, such as Pyrex ($\varepsilon = 5$) or ceramic ($\varepsilon \approx 10$), has effect of a virtually grounded electrode which further reduces the rf plasma potential at the fundamental and harmonics. Reduction of the rf plasma potential in ICP up to the level considerably less than electron temperature has been demonstrated in Ref. 7 by combination of the balanced coil drive and the ceramic window.

Next, we discuss an effective and simple way for reducing the rf plasma potential by splitting the coupler coil and inserting the resonating capacitor between the coil cuts. That allows considerable reduction of the maximal coil rf potential referenced to ground, while upholding the EMF that sustains the ICP. Additional benefits of the split coil configuration are reduced coupler loss and smaller conductive electromagnetic interferences (EMI).

Figure 2 shows traditional non-symmetric [Fig. (2a)] and symmetric [Fig. (2b)] drives of the coupler coil together with configurations having split coil couplers and the corresponding rf potential distribution, $V(x)$, along the coils. For all cases, $x = l$ corresponds to the input terminal and $x = 0$ to the grounded terminal. Figure 2(a) shows the coil rf potential for non-split coil configurations, same as in Figs. 1(b) and 1(c). In these configurations, the maximum coil potential is equal to the full coil voltage, $V_c = I_c[(\omega L)^2 + (R_0 + R_p)^2]^{1/2}$. At the

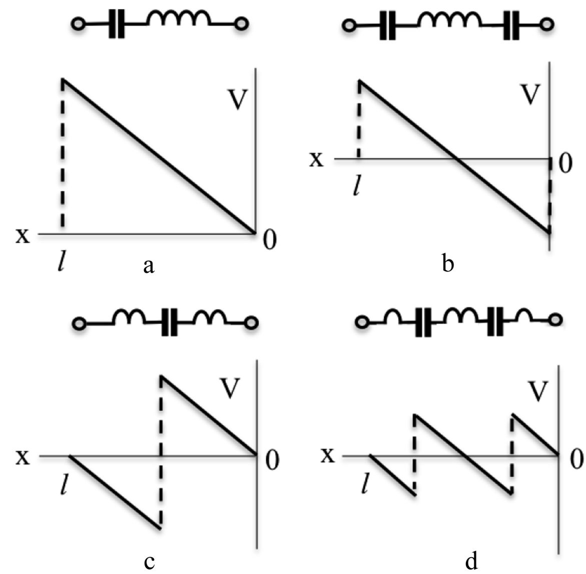

FIG. 2. The rf potential distribution along the coupler coil for different positions of resonating capacitors.

resonance frequency ($1/\omega C = \omega L$), this voltage, $V_c \approx -I_c/\omega C$, is shown in Fig. 2 by dashed lines. The input voltage, $V_a = I_c (R_0 + R_p) = I_c/\omega CQ \approx V_c/Q$, is considerably less than voltage across the coil and, therefore, is neglected in Fig. 2.

Figure 2(b) shows the (used in some commercial plasma reactors) configuration for partial balancing the coil potential for a non-balanced drive. There, each capacitor is twice the value of the resonating capacitance. At the resonance, the maximum coil potential referenced to ground is nearly a half of the coil voltage, V_c, shown in Fig. 2(a) for the unbalanced coil.

A similar result can be obtained by inserting a capacitor in the middle of the coil as shown in Fig. 2(c). Insertion of two equal capacitors with twice larger capacitance than the resonating capacitance, C, as shown in Fig. 2(d), leads to four times the reduction of the coil maximal rf potential. Additional coil splitting and insertion of additional capacitors allows further reduction of the coil rf potential.

Although the maximal coil rf potentials for the configuration in Figs. 2(b) and 2(c) are equal, the configuration in Fig. 2(c) has better suppression of the plasma rf potential comparing to Fig. 2(b). The rf potential distribution along the coil in Fig. 2(c) is such that those points with high rf potentials of opposite phase are at a short distance apart. That compensates the resultant capacitive coupling to plasma.

Splitting the coupler coil with inserted capacitors can partly symmetrize the coil rf potential at the non-symmetrical drive, but due to the final antenna Q-factor, one can reach (with proper choice of the coil braking points and capacitor values) rf voltage balance, but not phase balance, as it is the case for a true symmetrical drive. Connecting of the coil circuits [see Figs. 2(b)–2(d)] to a symmetrical (balanced) rf voltage source provides complete coupler balancing (in both voltage and phase).

Practical circuits for the non-symmetrical drive which significantly reduce the rf plasma potential are shown in Fig. 3(a) for capacitive matching[11] and in Fig. 3(b) for transformer matching.[6–8] The component values insuring matching to the

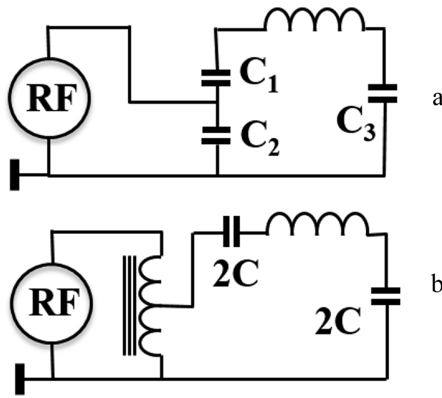

FIG. 3. Non-symmetrical drive providing partial balancing and significant reduction of the plasma rf potential for (a) capacitive matching and (b) transformer matching. The coil potential to ground is reduced to a half of the unbalanced version.

50 Ω rf generator of the capacitive network in Fig. 3(a) have to satisfy the following relations:

$$C^{-1} = C_1^{-1} + C_2^{-1} + C_3^{-1}, \quad C/C_2 = [(R_0 + R_p)/50]^{1/2},$$
$$(\omega C)^{-1} = \omega L. \tag{3}$$

Matching of the transformer network in Fig. 3(b) is arranged by selecting the transformer primary to the secondary turns ratio $N_1/N_2 = [50/(R_0 + R_p)]^{1/2}$.

Further reduction of the coupler coil rf potential is achieved in the circuit shown in Fig. 4 with true symmetrical drive. Here the coupler rf potential is reduced four times comparing to the conventional coil drive shown in Figs. 1(b), 1(c), and 2. This network also significantly reduces conductive EMI due to smaller capacitive coupling to the ground and increases the coupler Q-factor by reducing detrimental effect of stray capacitance.

The plasma rf potential, V_0, for the coupler configurations considered above was measured in 10 mTorr argon ICP within a cylindrical Pyrex chamber (OD = 134 mm, ID 126 mm) with two flat SS flanges separated by distance H = 120 mm.[12] In all cases, the rf power delivered to the coupler was 100 W at the frequency around 2.5 MHz, and the peak-to-peak coil electromotive force was about 2 kV.

A 10-turn (2.5 + 5.0 + 2.5 turns) coupler coil was wound around the chamber with AWG 16 Teflon insulated wire threaded through 2.5 mm OD Teflon tubing. This made the gap between the winding turns nearly equal to the wire

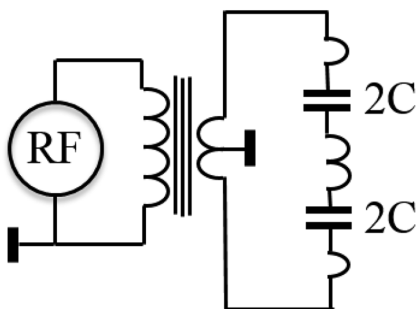

FIG. 4. Symmetrical transformer drive of the ICP split coil coupler with two capacitors.

diameter, thus maximizing the coil Q-factor, Q_0. This network comprising the split coil inductance and the capacitance, C = 200 pF, made of two 400 pF rf ceramic capacitors connected in series, resonated at a frequency ω/2π close to 2.5 MHz. The coupler was driven via the step-down transformer having a stepwise variable output resistance of 5.6, 8, 12.5, 17, and 22 Ω.

In the course of our experiment with different coupler configurations, the waveforms of the coil current, $\mathbf{I}_c(t)$, input voltage, $\mathbf{V}_a(t)$, and rf plasma potential, $\mathbf{V}_0(t)$, were acquired, and the coupler electrical parameters were calculated.

For characterization of the unloaded coupler of different configurations corresponding to Figs. 2(c)–2(d), the resonant frequency, f_{r0}, and Q-factor, Q_0, were found by measuring the coil current and voltage, $\mathbf{I}_c(t)$ and $\mathbf{V}a(t)$, at resonance condition, [$\omega L = (\omega C)^{-1}$ and $\phi = 0$]. Then, R_0, P_0, and Q_0 were found as follows:

$$R_0 = V_{a0}/I_{c0}, \quad P_0 = V_{a0}I_{c0}, \quad Q_0 = (\omega r_0 C R_0)^{-1}. \tag{4}$$

Values of Q_0 found this way for three different coupler configurations are given in Table I.

As is seen in Table I, the resonance frequency, f_{r0}, and Q-factor, Q_0, depend on the coupler configuration. Since both the coil inductance, L_0, and the resonating capacitance, C, were the same for all coupler configurations, we assume that the reason for such changes is the modified distribution of the rf potential along the coil which affects the stray capacitance impact on f_{r0} and Q_0.

Comparison of rf plasma potentials, V_0, for different coupler configurations, was performed by measuring this potential with a low capacitance rf voltage probe at a large surface area cylindrical electrode (l = 80 mm and OD = 3.6 mm) immersed into plasma.[13] The plasma potential waveform $\mathbf{V}_0(t)$ has pronounced fundamental and second harmonics. The fundamental harmonic in $\mathbf{V_p}(t)$ is due to some remnant imbalance of the coupler coil voltage, while the cause of the second harmonic is non-linearity of the wall sheath adjacent to the coupler coil.

The rule-of-the-thumb for the Langmuir probe plasma diagnostics calls for peak-to-peak rf plasma potential, $V_0 < T_e/e$; higher V_0 creates considerable distortion of the probe characteristic, thus, compromising the diagnostics. The unbalanced coupler in Fig. 1(c) creates the plasma potential 28 V (p-p) making impossible probe measurements without the adequate rf probe filter immersed into the plasma. The plasma rf potential, V_0, for balanced couplers presented in Figs. 2(b), 2(d), and 4 is well below T_e/e making possible Langmuir, B-dot, and microwave probe diagnostics without precaution related to perturbation caused by the rf plasma potential.

TABLE I. The coupler parameters and plasma rf potential.

Coupler configuration	f_{r0} (MHz)	Q_0	V_0, p-p (V)
1. Figure 1(c)	2.503	179	28
2. Figure 2(b)	2.559	194	1.5
3. Figures 2(d) and 4	2.581	230	1.0

In summary, we would like to emphasize the following:

1. Electrical characterization of ICP sources (and of other types, for this matter) is essential for finding the real power absorbed by plasma, P_p, coupler, P_0, and matcher, P_m, power losses. The power from rf generator, measured with an in-line power meter, $P_g = P_m + P_0 + P_p$, is always larger (and sometimes, significantly) than P_p, one which solely defines the plasma parameters and plasma effect in particular applications. Moreover, P_p/P_g is different for each specific apparatus and this ratio varies with changing rf power and gas pressure. That is why characterization of the plasma conditions by the power consumed from rf generator brings uncertainty and could be misleading.
2. There is a simple way to find plasma power, P_p, and power lost in the coupler, P_0, by measuring the coupler coil current, I_c, and power transferred to the coupler, P_t, with and without plasma. Such measurements (as well as ICP operation) do not require perfect tuning and matching. Detuning of the resonant circuit by $\Delta\omega = <\omega/Q$ and power reflection, $P_r/P_g < 30\%$ (if the rf generator tolerates it), are quite acceptable for accurate measurement of P_p and P_0.
3. Insertion of the resonating capacitor into the coupler coil considerably decreases the coil rf potential, thus, radically reducing the plasma rf and dc potentials and EMI. Those effects are enhanced by the symmetric coupler drive. This technique also increases the coupler Q-factor boosting the power transfer efficiency, facilitates ICP starting, and the ICP source ability to sustain stable discharge at low plasma density.

This work was partially supported by the DOE OFES (Contract No. DE-SC0001939).

[1] V. A. Godyak, "Ferromagnetic enhanced inductive plasma sources," J. Phys. D: Appl. Phys. **46**, 283001 (2013).
[2] S. Shinohara, Y. Miyauchi, and Y. Kawai, Plasma Phys. Controlled Fusion **37**, 1015 (1995).
[3] U. Eckert, "The hundred-year history of induction discharges," in Proceedings of the 2nd International Conference of Plasma Chemistry and Technology, 1984.
[4] Y. Yin, J. Messier, and J. A. Hopwood, "Miniaturization of inductively coupled plasma sources," IEEE Trans. Plasma Science **27**, 1516 (1999).
[5] R. Piejak, V. Godyak, and B. Alexandrovich, "A simple analysis of an inductive rf discharge,," Plasma Sources Sci. Technol. **1**, 179 (1992).
[6] V. Godyak, R. Piejak, and B. Alexandrovich, "Experimental setup and electrical characteristics of an inductively coupled plasma," J. Appl. Phys. **85**, 703 (1999).
[7] V. A. Godyak, "Electrical and plasma parameters of ICP with high coupling efficiency," Plasma Sources Sci. Technol. **20**, 025004 (2011).
[8] J. P. Rayner, A. D. Cheetham, and G. N. French, J. Vac. Sci. Technol. A **14**, 2048 (1996).
[9] J. Sevick, *Transmission Line Transformers* (American Radio Relay League, Inc., Newington, CT, 1990).
[10] J. Taillet, Am. J. Phys. **37**, 423 (1969).
[11] V. A. Godyak and B. M. Alexandrovich, "Plasma and electrical characteristics of inductive discharge in magnetic field," Phys. Plasmas **11**, 3553 (2004).
[12] J. Arancibia Monreal, P. Chabert, and V. Godyak, "Reduced electron temperature in a magnetized inductively-coupled plasma with internal coil," Phys. Plasmas **20**, 103504 (2013).
[13] V. A. Godyak and V. I. Demidov, "Probe measurements of electron energy distribution in plasma: What can we measure and how can we achieve reliable results?," J. Phys. D: Appl. Phys. **44**, 233001 (2011).